Tikrit Journal of Engineering Sciences (2022) 29 (4): 69-78
DOI: http://doi.org/10.25130/tjes.29.4.8

IRAQI Academic Scientific Journals

ISSN: 1813-162X (Print); 2312-7589 (Online)
Tikrit Journal of Engineering Sciences
available online at: http://www.tj-es.com

TJES Tikrit Journal of Engineering Sciences

Study the Affecting Factors on Free overfall Flow and Bed Roughness in Semi-Circular Channels by Artificial Neural Network

Raad Hoobi Irzooki [1], *Ayad Saoud Najem* [2]

1 Environmental Engineering Department, College of Engineering, Tikrit University, Tikrit, Iraq
2 Civil Engineering Department, College of Engineering, Tikrit University, Tikrit, Iraq

Keywords:

Artificial Neural Network ; Free overfall; Manning Roughness Coefficient; Semi-Circular Channels

ARTICLE INFO

Article history:
Received 27 Oct. 2022
Accepted 01 Dec. 2022
Available online 25 Dec. 2022

Citation: Irzooki RH, Najem AS. Study the Affecting Factors on Free overfall Flow and Bed Roughness in Semi-Circular Channels by Artificial Neural Network. Tikrit Journal of Engineering Sciences 2022; 29(4): 69-78.
http://doi.org/10.25130/tjes.29.4.8

Corresponding author:

Raad Hoobi Irzooki, E-mail: dr.raadhoobi@tu.edu.iq , Environmental Engineering Department, College of Engineering, Tikrit University, Tikrit, Iraq.

ABSTRACT

One of the significant problems facing the water resource engineer is calculating the coefficient of roughness for subsequent design calculations of the discharge amount of a channel or river. In this study, experiments were conducted in a semi-circular, straight channel to investigate the factors affecting bed roughness and flow discharge using Artificial Neural Network (ANN). For this purpose, three semi-circular channel models with free overfall were constructed and installed in a 6-meter-long laboratory flume. The length of these models was 2.50 m with three different diameters (D= 150, 187, and 237mm) and three bed slopes (S=0.004, 0.008, and 0.012). Three sand particle sizes (ds) were used for each semi-circular channel to roughen the bed. The results showed that the Manning roughness coefficient obtained using a rough bed surface was higher than the channel with a smooth bed surface. Also, the results revealed that the Manning roughness coefficient and the Froude number were inversely related. (ANN) analysis showed a good agreement between the experimental and predicted results of flow and roughness. The bring depth (y_b) had an 85.8% impact percentage on the free overfall discharge for semi-circular channels, while the bottom slope (S) had only 1.1%.

دراسة العوامل المؤثرة على مسقط الجريان الحر وخشونة القاع في القنوات نصف الدائرية باستخدام الشبكة العصبية الاصطناعية

رعد هوبي ارزوقي قسم هندسة البيئة/ كلية الهندسة / جامعة تكريت / تكريت - العراق.
أياد سعود نجم قسم الهندسة المدنية/ كلية الهندسة / جامعة تكريت / تكريت - العراق.

الخلاصة

واحدة من أكبر المشاكل التي تواجه مهندس الموارد المائية هي حساب معامل الخشونة لحسابات التصميم اللاحقة لكمية تصريف القناة أو النهر. في هذه الدراسة، أجريت التجارب في قناة مستقيمة نصف دائرية لاستقصاء العوامل المؤثرة على خشونة القاع وتصريف الجريان باستخدام الشبكة العصبية الاصطناعية (ANN). لهذا الغرض، تم إنشاء ثلاثة نماذج لقنوات نصف دائرية ذات مسقط حر وتم تثبيتها في قناة مختبرية بطول 6 أمتار. جميع نماذج هذه القنوات بطول 2.50 متر وبأقطار مختلفة (D=150, 187, and 237) ملم، مع ثلاثة ميول لقاع القناة (S= 0.004, 0.008 and 0.012). تم استخدام ثلاثة أحجام لحبيبات الرمل (ds) لكل نموذج من القنوات نصف الدائرية لتخشين طبقة قاع القناة. أظهرت النتائج أن معامل مانينغ للخشونة (n) الذي تم الحصول عليه باستخدام سطح قاع خشن أعلى من قيمته في القناة ذات سطح القاع الأملس. كما أوضحت النتائج وجود علاقة عكسية بين معامل مانينغ للخشونة ورقم فرود. أظهر تحليل (ANN) اتفاقًا جيدًا بين النتائج المختبرية والمتوقعة لتصريف الجريان والخشونة، وإن عمق الجريان عند نقطة السقوط الحر (yb) له نسبة تأثير 85.8 ٪ على تصريف الجريان الحر للقنوات نصف دائرية، بينما ميل القاع كانت نسبة تأثيره 1.1٪ فقط.

الكلمات الدالة: معامل مانينغ للخشونة، القنوات نصف الدائرية، المسقط الحر، الشبكة العصبية الاصطناعية.

1.INTRODUCTION

Roughness data is often limited or unavailable, especially in flood situations. Therefore, one of the tasks of the water resource engineer is to estimate the roughness values of the river, waterway, or channel. Then the engineer can use these values to calculate discharge, which is used as a basis for the values adopted in this study. Buffington and Montgomery (1999) noted that determining the Manning roughness coefficient (n) has become more difficult for engineers and researchers because the values of this coefficient cannot be calculated consistently for all sorts of open channels [1]. Guo et al. (2008) showed that, for a particular bed roughness size, the relative spacing of roughness, defined as the ratio of the center-to-center distance to the height of the strip, had a significant impact on the flow [2]. Bilgil and Altun (2008) used ANN to forecast the friction factor in a smooth open channel flow [3, 4]. Sadeque et al. (2009) presented the findings of an experimental investigation of flow around cylindrical objects on a rough surface in an open channel [5]. Mohammed et al. (2011) investigated the impact of bed roughness on the flow depths of free overfall (normal, critical, and brink depth). This research revealed that complete bed roughness significantly impacted on steeper slopes [6]. Devkota et al. (2012) investigated the relationship between water depth under low-flow circumstances, Manning's roughness coefficient, and water depth in partly filled culverts [7]. Mohammed-Ali (2012) investigated the hydraulic properties of sharp-crested weirs with a semielliptical shape. The study's dimensional analysis was supported by experimental work. The findings of the dimensional study showed that the ratios of the water height above the weir's crest to its short and long radiuses to its height (P/H) were the parameters that significantly influenced the discharge of flow over this type of weir. The results demonstrated very high agreement with the experimental result for calculating the discharge with knowledge of the weir's long and short-cutting radius (a) and (b), as well as the height of the crest (P) [8]. Ahmad et al. (2017) investigated the channel with a gravel bed surface. The results showed that the channel with a gravel bed surface had more significant flow resistance than the channel without a gravel bed surface. The flow pattern was considered subcritical since the Froude number for both situations in the flume was less than 1. In conclusion, it was determined that the kind of bed roughness, flow rate, and channel slope impacted the hydraulic roughness [9]. Mohammed (2018) investigated the critical depth and discharge model, free overfall utilizing a feed-forward back-propagation kind of neural network, and the multi-nonlinear regression model using statistical programming. For this purpose, 215 sets of experimental data for training and validation were used. The trained, validated, and tested neural network model outcomes were compared to the data collected in the lab. The calculated values were in good agreement with the measurements [10]. Irzooki and Hasan (2018) presented the results of a laboratory study on the properties of free overfall in rough and smooth triangular channels. In this experimental investigation, the authors examined four channel bed slopes (zero, 0.0041, 0.0082, and 0.0123), channel side slopes (0.8H:1V, 1H:1V, and 1.33H:1V), and

three roughness components in which the channel was roughened with gravel of varying sizes (1.18, 2.36, and 4.75 mm) for Froude numbers between 0.31 and 1.47 [11]. Jahanpanah et al. (2019) used an artificial neural network (ANN) and three additional soft computing models to predict the flow through rectangular channels. The models employed data from previously published research. Compared to other approaches, the ANN model's performance was better [12]. Ahmad et al. (2020) conducted experiments in a rectangular compound flume with fixed and nonaggregated bedding to assess the bed roughness as well as flow characteristics of the open rectangular channel. There were five sections of the flume. Crushed, coarse aggregates, and a clear channel were tested. The values calculated from the data collected throughout the investigation were between 0.008 and 0.018 for the clear channel, 0.013 and 0.030 for crushed aggregate, and 0.016 and 0.041 for coarse aggregate that was crushed [13]. The present paper concentrated on influencing factors on the flow and bed roughness in semi-circular channels. Artificial Neural Network (ANN) was used with experimental data to understand how the characteristics of semi-circular channels affect the roughness coefficient since it is one of the key variables in determining the flow characteristics in open channels.

2.METHODOLOGY

The work of this research was divided into two main parts, which are as follows:

2.1.Experimental work

2.1.1.Laboratory flume and semi-circular channel models

Experiments were carried out at the Hydraulic Laboratory of the Environmental Engineering Department at Tikrit University. This study was conducted in a 6 m long, rectangular flume with a cross-section of 0.3 m in width and 0.4 m in height. The flume's walls were made of Plexiglass, and the bed was made of painted iron, as shown in Fig. 1.

Fig. 1 Laboratory flume.

Each test used a PVC pipe to construct the semi-circular free overfall channel models. (D1, D2, and D3) represented semi-circular channels with 150, 187, and 237 mm diameters, respectively. The channel structure was made using square-shaped iron sections of dimensions (1×1) inch to fix the semi-circular channel at the height of 200 mm from the bed of the laboratory flume. This height was selected to ensure a free vertical drop at the model's end. The bottom of the channel was supported along with the structure by adjustable supports. The adjustable supports were used to avoid getting bends and curvatures of the channel bed during the experiments, as shown in Fig. 2.

Fig. 2 Steel frame for supporting the semi-circular channels.

n_0 denotes the roughness of the channel bed without any roughing material, while n_1, n_2, and n_3 denote the roughness of the channel bed with sand grain sizes (d_s) of 1.18, 2.36, and 4.75 mm, respectively. S_0 is the horizontal bed slope, whereas S_1, S_2, and S_3 are the semi-circular channel bed slopes, which were (1/250=0.004), (2/250=0.008), and (3/250=0.012), respectively. For each case of this study, four distinct discharges were passed.

2.1.2.Create the roughness of the channel bed

Three sand particle sizes (ds) were used to roughen the bed for each channel model, as shown in Fig. 3. This roughness was fixed by applying adhesive paper to the channel's bed and then gluing the roughness to the sticky paper, as illustrated in Fig. 4.

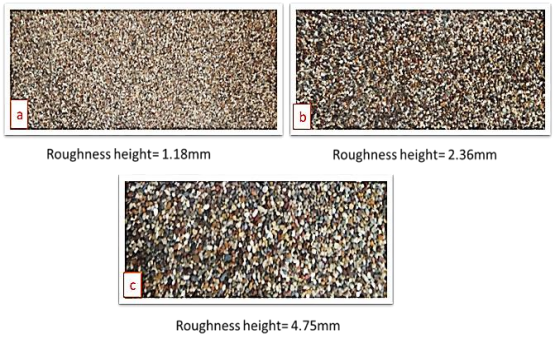

Fig. 3 Bed roughness materials.

Fig. 4 Stages of installing the roughness layer

2.1.3.Water depth measurement

Two-point gauge scales with an accuracy of 0.1 mm were used to measure the depth of the water. One was used to measure the water depth along the semi-circular channel, and the other was used to measure the depth of the water over the triangular weir to calculate the discharge passing through each experiment. Fig. 5 shows a 90-degree V-notch weir with a sharp crest used to measure the channel discharge. This weir was constructed with 10 mm thick Plexiglass. The rate of these discharges was calculated using the following discharge equation for a weir with a triangular opening [14].

$$Q = 0.012\ H^{2.552} \quad \textbf{(1)}$$

Q is the rate of discharge (ℓ/sec), and H is the depth of water over the weir crest (cm).

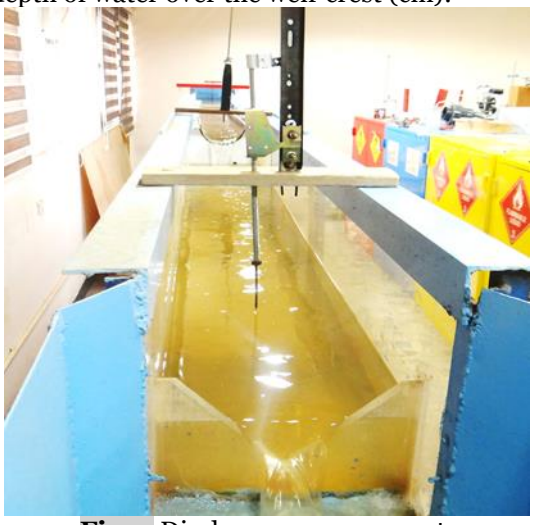

Fig. 5 Discharge measurement.

The water's depth was measured depending on the material used for constructing the channel bed. The following two methods can be used to determine the depth:

1.Depth measurement in smooth channels

Water flows uniformly through the bed of smooth channels at their upstream edges; hence the level of the bed was used as a direct reference when measuring the depth of the flow.

2.Depth measurement in rough channels

The flow over the channel's rough bed was non-uniform, as the depth varied continuously with the flow direction. To approximate the state of the flow in channels to the state of uniform flow, a uniform level of height for the bed of the channel was chosen, which was adopted as an actual line to measure the depth of flow. Schlichting (1937) conducted his conception regarding the geometrical bottom level of the channel. Schlichting considered that all the roughness models melted into the form of a smooth bottom, and the surface level was used as the actual level of measurement [15]. Morris (1959), who relied on that, considered that the highest level of roughness was the level of the bottom [16]. According to Gordienko (1967),

the designed depth was more significant than the top of a rough surface, which was less than the calculated depth of the lower bottom of the channel structure ($h + y_e > y > y_e$) [17]. In his study on rough channels with zigzag beams when (L/h is greater than 1.414), the channel's design depth (y) was:

$$y = y_e + h - \frac{2h^2}{l^2} \quad \textbf{(2)}$$

where y_e is the measurement of flow depth taken from the highest point of the roughness components, h is the roughness components' height, and L is the longitudinal distance from the center to the center of the roughness components. The flow depth was measured in the present study, as shown in Fig. 6. The geometric mean of a bottom level was used as the actual level for measuring the normal depths upstream of the edge area:

$$y = \frac{y_{e+(y_e+h)}}{2} = y_e + \frac{h}{2} \quad \textbf{(3)}$$

where y_e is the measurement of flow depth was taken from the highest point of the roughness components to the top water surface level, and h is the height of the roughness component (the distance from the bottom of the channel to the top of the roughness components).

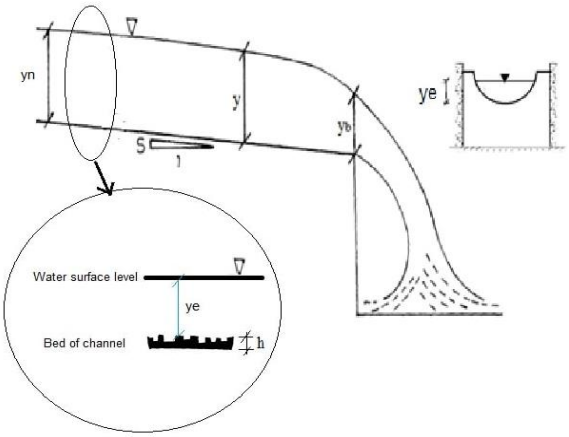

Fig. 6 Depth measurement in semi-circular channels.

2.2.Artificial Neural Network Modeling

An artificial neural network is a powerful modeling technique for datasets with nonlinear relationships between variables. An essential function of ANNs is data analysis with many inputs and outputs. Sets for identifying and training correlated input patterns and data pairs for output are the most vital component of modeling using (ANN), allowing for extrapolation and predicting results from new data sets for input. In a network structure based on (ANN), neurons are structured in three layers in a completely integrated pattern: the input layer, the hidden layers, and the output layer are all present. Neurons present an input layer that gets information from a data file. Neurons present publish the network's reaction to the input data at the output layer. Neurons in the hidden layer perform the data processing. A method of communication between neurons separated into three different layers creates a framework, either a pattern or a network, from which a solution may be derived. According to the theory, approximating most functions is as simple as only one covert level [18]. (ANN) modeling has been gaining popularity and utilized as an advanced computational tool in numerous disciplines of water resources engineering. Several authors, including (Dolling and Varas, 2002) [19], (Sahu et al., 2011) [20], and (Jamel, 2018) [21], explored the use of (ANN) modeling for the prediction of flow parameters.

2.2.1.Implementing Artificial Neural Networks

An ANN model consists of an input layer, hidden layer, and output layer that are linked in some way [4]. One or even more hidden layers may be formed by connecting the nodes of the input and output layers. No two neurons in the same layer are connected; however, all neurons in the same layer are linked to all neurons in the next layer Fig. 7. Data taken in by the input layer is processed in the hidden layer and then output to either a class label or a continuous value prediction. Each value from the input layer that passes through a hidden node is multiplied by a set of predefined integers called weights, and the sum of these products is the output. The obtained value is then used as the input into a nonlinear mathematical function called the activation function, which returns a value between zero and one. In Fig. 8, Eqs. 4 and 5 represent the net sum of the weighted inputs entering a node j and the output activation function that converts a neuron's weighted input to its output activation (the most usually used is the sigmoid function).

$$S_j = \sum_{i=1}^{n} x_i w_{ij} \quad \textbf{(4)}$$

$$O_j = \frac{1}{1+e^{S_j}} \quad \textbf{(5)}$$

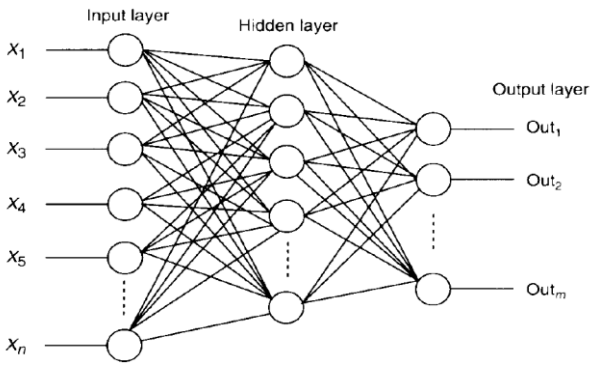

Fig. 7 Neural network architecture.

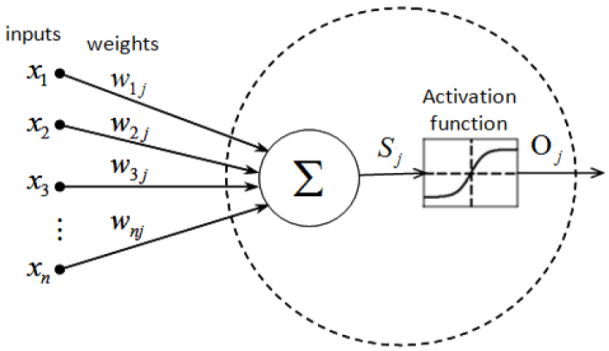

Fig. 8 Active node.

Neurons, and by implication ANNs, may either be in "training mode," where they are being learned, or in "using mode," where they are being applied. Train the system to anticipate outputs, inputs, and results from a real-world data set will be utilized during the training phase. This kind of supervised learning starts with randomly generated weights and then uses gradient descent search techniques like Backpropagation to perfect them for the specific job. The error function uses the discrepancy between the desired and actual output values to motivate improvement.
It is necessary to adjust the weights to minimize the error, which in turn affects the error function. An error in a neuron's output may be described as follows:

$$E_j = \frac{1}{2}(O_j - t_j)^2 \quad \textbf{(6)}$$

The given training set $\{(x_1, t_1), (x_2, t_2), \ldots, (x_k, t_k)\}$ consists of k-ordered pairs of n inputs and m dimensional vectors (n-inputs, m-outputs), also known as the input and output patterns. Whereas the network's error function, which must be minimized, is defined as:

$$E_j = \frac{1}{2}\sum_{j=1}^{k}(O_j - t_j)^2 \quad \textbf{(7)}$$

where t_j is the desired value, and O_j is the output generated by the network when fed the input pattern x_j from the training set. A value of $\Delta w_{ij} = -\gamma \frac{\partial E}{\partial w_{ij}}$ adjusts each weight throughout training, where g is a constant that represents the learning rate. However, the search route may get imprisoned around the ideal solution if the learning rate is too high, making convergence impossible. Once a decent weight set has been determined, the neural network model can automatically forecast the outputs for a new dataset whose values are unknown [22]. The (ANN) model was developed utilizing the database of experimental results. The developed model links the output variables to the input variables. The variables used to build the (ANN) to study the factors affecting the discharge and roughness are shown below.

2.2.2.Data for factors that affect discharge over free overfall of a semi-circular channel

The neural network model was developed and validated using the Multilayer Perceptron (MLP) Module of IBM SPSS Statistics 26. Multilayer Perceptrons (MLPs) are neural networks trained to utilize a back-propagation learning technique that uses gradient descent to update the weights to minimize the error function. All variables were normalized to the range 0-1 using the formula (x–min)/(max–min), and only data from the training set was used in the training process. About 74% of the observed experimental data were examined as training samples in the processing of (ANN), while the remaining 26% were examined as testing samples, as shown in Table 1. The parameters (y_b, D, S, n) are the input variables, while the discharge (Q) is the output variable, where (y_b) is the bring depth.

Table 1 Processing summary of the ANN model

Details		N	Persent
Sample	Training	80	74.1%
	Testing	28	25.9%
Vaild		108	100%
Excluded		0	-
Total		108	-

The (ANN) model enables users to choose the number of hidden layers as well as the maximum and minimum units that may be chosen for each hidden layer. The most effective number of units in the hidden layer was determined using the automated architecture. Fig. 9 illustrates how automatic architecture selection utilizes the preset activation functions of the hidden and output layers. Where the bias node of a neural network is the number added to the sum of the features and the weights. The purpose is to counteract the effect, And it aids models in changing the activation function to the positive or negative value.

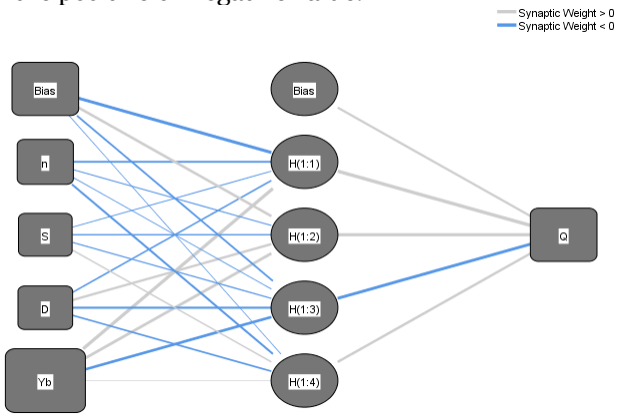

Fig. 9 Activation function of a hidden layer for free overfall discharge of semi-circular channel.

2.2.3.Data for factors that affect the Manning roughness coefficient of a semi-circular channel

About 68.5% of the observed experimental data were examined as training samples in the processing of (ANN), while the remaining 31.5% were examined as testing samples, as shown in Table 2. The parameters (y_n, D, S, Q) are the input variables, the Manning roughness coefficient (n) is the output variable, and y_n is the normal depth.

Table 2 Processing summary of Manning Roughness Coefficient ANN model

Details		N	Persent
Sample	Training	74	68.5%
	Testing	34	31.5%
Vaild		108	108
Excluded		0	-
Total		108	-

The network architecture used is a multilayered network architecture (multilayer). The network diagram used by SPSS to predict the course outcome for the Manning roughness coefficient is shown in Fig. 10 below.

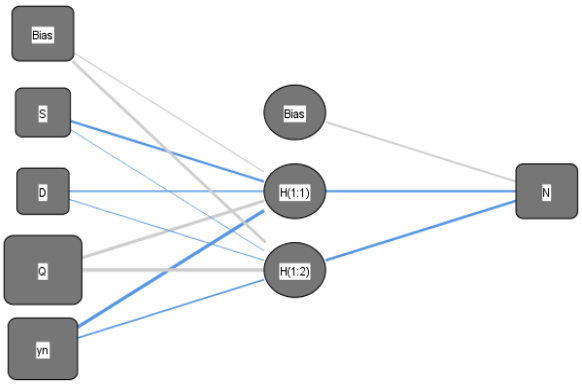

Fig. 10 Activation function of a hidden layer for Manning (n) of semi-circular channel.

3.RESULTS AND DISCUSSION

Overall, 192 tests were made of flow in the semi-circular channels. The range of tested discharges was between 0.000198 and 0.005267 m^3/hr.

3.1.Determine the Manning roughness coefficient values

The values of the normal depth and discharge were found in each experiment. Manning's equation was used to evaluate the correct values of manning's roughness coefficient based on the models of the bed roughness for all cases, as follows:

$$n = \frac{KR^{2/3}S^{1/2}}{(Q/A)} \quad \textbf{(8)}$$

Since K = constant is equal to 1 when Eq. 8 is in the international system (SI), K=1.49 when Eq. 8 is in the British units, n is Manning's roughness coefficient ($s/m^{\frac{1}{3}}$), Q is flow discharge (m^3/s), V is flow velocity (m/s), R is the hydraulic radius (m) = A/p_w, A is the area of flow cross-section (m^2), p_w is wet perimeter (m), and S is the channel bed slope. An average parameter (n) value was found for each roughness model with different bottom inclinations, which was classified in Table 3.

Table 3 Manning's roughness coefficient

d_s mm	D1=150 mm		D2=187 mm		D3=237 mm		Average n
1.18	n1	0.01958	n1	0.01572	n1	0.01863	0.01797
2.36	n2	0.02198	n2	0.01832	n2	0.02251	0.02094
4.75	n3	0.034398	n3	0.02526	n3	0.02309	0.027584

Table 3 illustrates the importance of the conception that the most significant roughness appeared for a grain size of 4.75 mm for the third model, in which Manning's coefficient value of roughness (n) equals 0.027584. It is shown that the effect of roughness increased as the grain size increased, although the roughness coefficient value was taken as an average for several cases. The rate of change of Manning's roughness coefficient values (n) with sand grain size (d_s) used as channel roughness (for grain diameters, d_s = 1.18 mm, 2.36 mm, and 4.75 mm) is represented in Fig. 11.

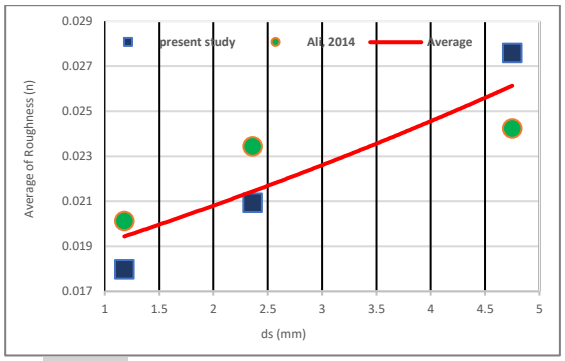

Fig. 11 Manning's roughness coefficient.

The obtained results were compared with the results of Ali (2014), who used a rough triangular channel with the same sand grain size used in this study [23]. From Fig. 11, the coefficient of determination (R^2) equals 0.7873. There is apparent convergence in the results, and there may be a little difference due to the different channel shapes and the flows passing through the channel.

3.2.Effect of the channel slope and diameter on the Manning roughness coefficient

The relationship between the bed slope of a semi-circular channel with a diameter of 0.237 m and the average Manning roughness coefficient is shown in Fig. 12. This figure shows that for a channel with a similar roughness material, the roughness coefficient increased as the channel bed slope increased. Additionally, the roughness coefficient increased with increasing the size of roughened material for the channel, which is consistent with what was found by Devkota et al. (2012) [7]. The same results were observed for channels with

diameters (0.187 and 0.150 m), as shown in Figs. (13, 14), respectively. It is important to note that, while the bed slope and roughened material were constant, it seems from these figures that the roughness coefficient increased with decreasing the channel diameter.

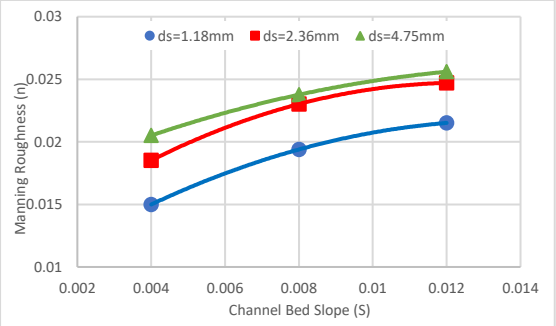

Fig. 12 Effect of bed slope on Manning's roughness coefficient for a semi-circular channel with a diameter of 0.237m.

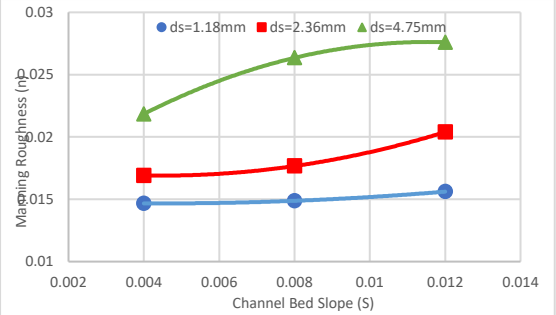

Fig. 13 Effect of bed slope on Manning's roughness coefficient for a semi-circular channel with a diameter of 0.187m.

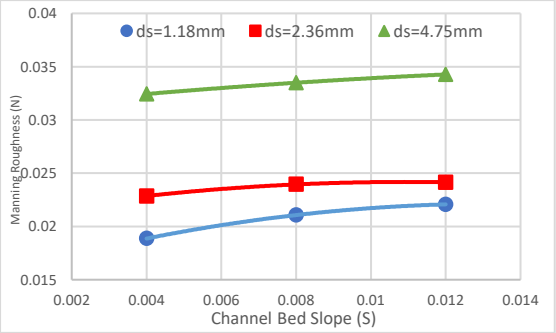

Fig. 14 Effect of bed slope on Manning's roughness coefficient for a semi-circular channel with a diameter of 0.15m.

3.3.Effect of the Manning roughness coefficient on the Froude Number

The relationship between the Froude number and Manning's roughness coefficient for channels with diameters of 0.187 m and 0.237 m that passed a discharge of 0.0042 m3/sec is shown in Fig 15. This figure demonstrates the Manning roughness coefficient decreases with increasing Froude Number. In addition, this figure disply an inversely related between the Manning roughness coefficient and the diameter of the channel, where this coefficient increases with decreasing the channel diameter for the same Froude Number.

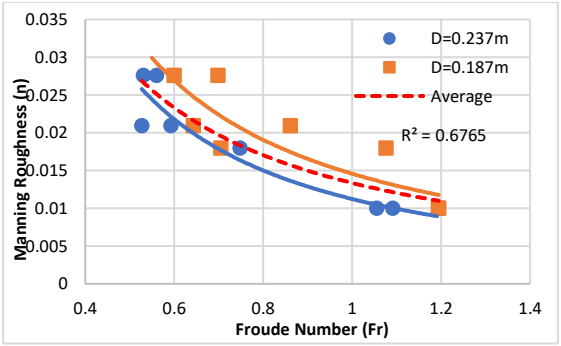

Fig. 15 Relationship between Manning roughness coefficient and Froude Number.

3.4.Analysis the results using ANN model for discharge

The sum of squares error for Training was 1.319, and the relative error was 0.036. For testing, the sum of squares error for Training was 1.087, and the relative error was 0.065. The parameter estimates are listed in Table 4.

Table 5 displays the relative weights of the input variables. As can be seen, the bring depth (y_b) had a significant percentage of 85.8%, making it the parameter that had the most significant impact on discharge over a semi-circular channel free overfall. Additionally, the bottom slope relevance percentage was only 1.1%. The comparison between predicted values of (Q) by ANN and experimental values agreed with the coefficient of determination (R^2), equaling 0.9521, as shown in Fig. 16.

Table 4 Parameter estimates for Discharge

Predictor		Predicted Hidden Layer 1				Output Layer
		H(1:1)	H(1:2)	H(1:3)	H(1:4)	Q
Input Layer	(Bias)	-0.472	0.675	-0.003	-.0360	
	n	0.189	0.140	0.052	0.168	
	S	0.190	0.041	-0.104	-0.436	
	D	-0.555	-0.234	.0362	-0.467	
	Yb	-0.162	-0.745	-0.836	0.305	
Hidden Layer 1	(Bias)					0.263
	H(1:1)					-0.359
	H(1:2)					-0.976
	H(1:3)					-0.772
	H(1:4)					0.011

Table 5 Importance percentage of input variables on discharge over free overfall of semi-circular channel

Independent Variable	Importance	Normalized importance
n	0.092	10.7%
S	0.011	1.3%
D	0.040	4.6%
y_b	0.858	100.0%

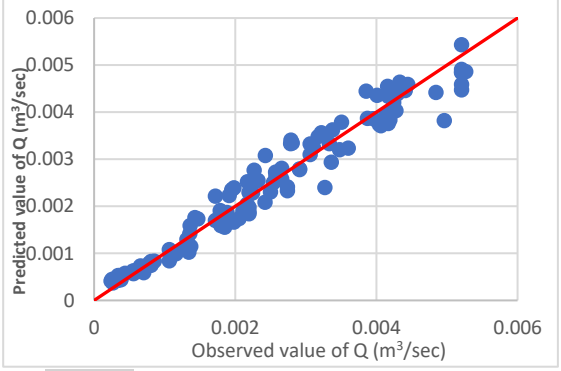

Fig. 16 Comparison between predicted and observed discharge over free overfall of semi-circular channel.

3.5.Analysis of the results using the ANN model for the Manning roughness coefficient

The sum of squares error for training was 2.943, and the relative error was 0.081. For testing, the sum of squares error for training was 1.130, and the relative error was 0.070. The parameter estimates are listed in Table 6.

Table 6 Parameter Estimates for Manning roughness coefficient

Predictor		Predicted		
		Hidden Layer 1		Output Layer
		H(1:1)	H(1:2)	N
Input Layer	(Bias)	.212	1.414	
	S	-.969	-.077	
	D	-.457	-.199	
	Q	1.515	2.182	
	yn	-1.881	-.611	
Hidden Layer 1	(Bias)			.697
	H(1:1)			-.912
	H(1:2)			-1.176

The result of the analysis of factors affecting the roughness coefficient of semi-circular channels by ANN is presented in Table 7. The discharge had a significant percentage of 44.6%, making it the parameter that had the most significant impact on the Manning roughness coefficient of the semi-circular channel free overfall. Additionally, the bottom slope relevance percentage was only 13.2%.

Table 7 Importance percentage of input variables on Manning roughness coefficient of the semi-circular channel

Independent Variable	Importance	Normalized importance
S	0.132	29.5%
D	0.091	20.4%
Q	0.446	100.0%
yn	0.331	74.2%

The comparison between predicted values of (n) by (ANN) and experimental values gave a good agreement with the coefficient of determination (R^2) equaling 0.9232, as shown in Fig 17.

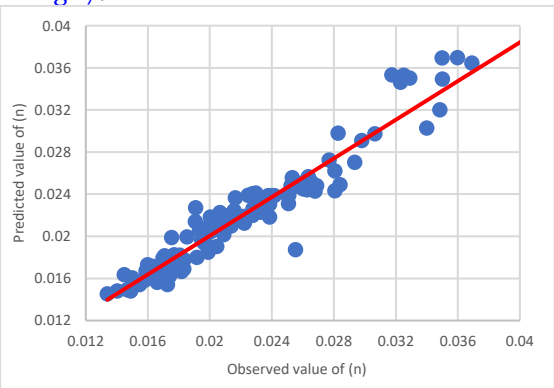

Fig. 17 Comparison between predicted and observed n for semi-circular channel.

4.CONCLUSIONS

The present study investigated the flow characteristics of semi-circular channels with free overfalls. The experiments included passing different flows through channels with variable bed slopes, diameters, and bed roughness. Based on the analysis of the results of 192 tests, the following are the most significant findings of this study:

1. The roughness coefficient increased as the channel bed slope increased.
2. The roughness coefficient increased with increasing the size of roughened material for the channel.
3. The roughness coefficient increased with decreasing channel diameter.
4. The Manning roughness coefficient decreased with increasing Froude Number. An inverse relation between the Manning roughness coefficient and the diameter of the channel was found. In contrast, the Manning roughness coefficient increased with decreasing the channel diameter for the same Froude Number.
5. (ANN) analysis showed a good agreement between the experimental and predicted results. The bring depth (y_b) had the most significant impact on the discharge of free overfall for a semi-circular channel with a percentage of 85.8%, while the bottom slope (S) had a minimum impact with a percentage of only 1.1%.
6. Good agreement was observed between the (n) values predicted by the (ANN) and the experimental values. The discharge was the characteristic that most affected the Manning roughness coefficient of the semi-circular channel's free overfall.

REFERENCES

[1] Buffington JM, Montgomery DR. **Effects of hydraulic roughness on surface textures of gravel-bed rivers**. *Water Resources Research* 1999; **35**(11):3507–3521.

[2] Guo Y, Zhang L, Shen Y, Zhang J. **Modeling Study of Free Overfall in a Rectangular Channel with Strip Roughness**. *Journal of Hydraulic Engineering* 2008; **134**(5):664–667.

[3] Bilgil A, Altun H. **Investigation of flow resistance in smooth open channels using artificial neural networks**. *Flow Measyrement and Instrumentation* 2008; **19**(6):404–408.

[4] Yuhong Z, Wenxin H. **Application of artificial neural network to predict the friction factor of open channel flow**. *Communications in Nonlinear Science and Numerical Simulation* 2009; **14**(5):2373–2378.

[5] Sadeque MA, Rajaratnam N, Loewen MR. **Effects of bed roughness on flow around bed-mounted cylinders in open channels**. *Journal of Engineering Mechanics (ASCE)* 2009; **135**(2):100–110.

[6] Mohammed MY, Al-taee AY, Al-Talib AN.

Gravel Roughness and Channel Slope Effects on Rectangular Free Overfall. *Damascus University Journal* 2011; **27**(1):47–54.

[7] Devkota JP, Baral D, Rayamajhi B, Tritico HM. **Variation in manning's roughness coefficient with diameter, discharge, and slope in partially filled HDPE Culverts**. *World Environmental and Water Resources Congress: Crossing Boundaries* 2012: 1716–1726.

[8] Mohammed-Ali WS. **Hydraulic Characteristics of Semi-Elliptical Sharp Crested Weirs**. *International Journal Review of Civil Engineering* 2012; **3**: 42-46.

[9] Ahmad NA, Bahry SIS SI, Ali ZM, Daud AMM, Musa S. **Effect of Flow Resistance in Open Rectangular Channel**. *MATEC Web of Conferences*, 2017;97.

[10] Mohammed AY. **Artificial Neural Network (ANN) Model for End Depth Computations**. *Journal of Civil and Environmental Engineering* 2018; **8**(3):2-5.

[11] Irzooki R, Hasan S. **Characteristics of flow over the free overfall of triangular channel.** *MATEC Web of Conferences*, 2018; 162:1–6.

[12] Jahanpanah E, Khosravinia P, Sanikhani H, Kisi O. **Estimation of discharge with free overfall in rectangular channel using artificial intelligence models**. *Flow Measurement and Instrumentation* 2019; **67**:118–130.

[13] Ahmad NA, Hadzim MF, Musa S. Experimental Study for Determination of Bed Roughness in Open Rectangular Channel. *IOP Conference Series: Earth and Environ Science* 2020; 498.

[14] Irzooki RH, Yass MF. **Hydraulic Characteristics of Flow Over Triangular Broad Crested Weirs Hydraulic Characteristics of Flow Over Triangular Broad Crested Weirs.** *Engineering and Technology Journal* 2015; **33**(7): 86–96

[15] Schlichting H. *Experimental investigation of the problem of surface roughness*. National Advisory Commitee for Aeronautics, 1937.

[16] Morris HM. **Design methods for flow in rough conduits**. *Journal of the Hydraulics Division (ASCE)* 1959; **85**(HY7):43–62.

[17] Gordienko PI. **The influence of channel roughness and flow states on hydraulic resistances of turbulent flow**. *Journal of Hydraulic Research* 1967; **4**:249–261.

[18] Ripley BD. *Neural Networks and Pattern Recognition*. New York Cambridge Univ. Press, 1996.

[19] Dolling OR, Varas EA. **Artificial neural networks for streamflow prediction**. *Journal of Hydraulic Research* 2002; **40**(5):547–554.

[20] Sahu M, Khatua KK, Mahapatra SS. **A neural network approach for prediction of discharge in straight compound open channel flow**. *Flow Measurement and Instrumentation* 2011; **22**(5):438–446.

[21] Jamel AA. **Numerical simulation for estimating energy dissipation over different types of stepped spillways and evaluate the performance by Artificial Neural Network.** *Tikrit Journal for Engineering Sciences* 2018; **25**(2):18-26.

[22] IBM SPSS Neural Networks 22 manual.

[23] Ali SIH. *Experimental Study for Characteristics of Flow in Triangular Channels with Free Over Falls*. M.Sc. Thesis, College of Engineering-Tikrit University, 2014.